Neurobiology of Disease 130 (2019) 104520

Contents lists available at ScienceDirect

Neurobiology of Disease

journal homepage: www.elsevier.com/locate/ynbdi

ER responses play a key role in Swiss-Cheese/Neuropathy Target Esterase-associated neurodegeneration

Sunderhaus Elizabeth R.[1], Law Alexander D., Kretzschmar Doris*

Oregon Institute of Occupational Health Sciences, 3181 SW Sam Jackson Park Rd., Portland, OR 97239, United States of America

ARTICLE INFO

Keywords:
Unfolded protein response
Patatin-like phospholipase domain-containing protein 6
Sarco/endoplasmic reticulum Ca2+ ATPase
Lipid homeostasis
Spastic paraplegia/ataxia
Organophosphate-induced delayed neuropathy

ABSTRACT

Swiss Cheese (SWS) is the *Drosophila* orthologue of Neuropathy Target Esterase (NTE), a phospholipase that when mutated has been shown to cause a spectrum of disorders in humans that range from intellectual disabilities to ataxia. Loss of SWS in *Drosophila* also causes locomotion deficits, age-dependent neurodegeneration, and an increase in lysophosphatidylcholine (LPC) and phosphatidylcholine (PC). SWS is localized to the Endoplasmic Reticulum (ER), and recently, it has been shown that perturbing the membrane lipid composition of the ER can lead to the activation of ER stress responses through the inhibition of the Sarco/Endoplasmic Reticulum Ca^{2+} ATPase (SERCA). To investigate whether ER stress induction occurs in NTE-associated disorders, we used the fly *sws* null mutant as a model. *sws* flies showed an activated ER stress response as determined by elevated levels of the chaperone GRP78 and by increased splicing of XBP, an ER transcription factor that activates transcriptional ER stress responses. To address whether ER stress plays a role in the degenerative and behavioral phenotypes detected in sws^1, we overexpressed XBP1, or treated the flies with tauroursodeoxycholic acid (TUDCA), a chemical known to attenuate ER stress-mediated cell death. Both manipulations suppressed the locomotor deficits and neurodegeneration of sws^1. In addition, sws^1 flies showed reduced SERCA levels and expressing additional SERCA also suppressed the sws^1-related phenotypes. This suggests that the disruption in lipid compositions and its effect on SERCA are inducing ER stress, aimed to ameliorate the deleterious effects of sws^1. This includes the effects on lipid composition because XBP1 and SERCA expression also reduced the LPC levels in sws^1. Promoting cytoprotective ER stress pathways may therefore provide a therapeutic approach to alleviate the neurodegeneration and motor symptoms seen in NTE-associated disorders.

1. Introduction

Neuropathy Target Esterase (NTE) belongs to the family of patatin-like phospholipase domain-containing proteins (PNPLA), a family of hydrolases that in mammals consists of at least eight members (Kienesberger et al., 2009). PNPLA family members show specific activity against diverse substrates, including phospholipids, triacylglycerols, and retinol esters, and they are expressed in various tissues. NTE, also called PNPLA6, was shown to preferably hydrolyze phosphatidylcholine (PC) and lysophosphatidylcholine (LPC) (Lush et al., 1998; Quistad et al., 2003; van Tienhoven et al., 2002). NTE is widely expressed in the developing and adult nervous system, but its expression becomes more restricted to large neurons with age (Glynn et al., 1998; Moser et al., 2000). Loss of NTE in mice causes lethality during embryogenesis due to placental defects and impaired vasculogenesis (Moser et al., 2004) while a brain specific deletion is viable, but when aged these mice show neuronal degeneration and defects in motor coordination (Akassoglou et al., 2004). In humans, mutations in NTE have been connected with a variety of diseases including NTE-related motor neuron disorder, Boucher-Neuhäuser, Gordon-Holmes, and Oliver McFarlane Syndrome to name a few (Deik et al., 2014; Kmoch et al., 2015; Rainier et al., 2011; Synofzik et al., 2014; Topaloglu et al., 2014). These are complicated autosomal recessive diseases with varying clinical symptoms such as hypogonadism, chorioretinal dystrophy, ataxia, and spasticity. While mutations in NTE have been shown to cause the disease in the affected patients, the underlying molecular mechanism are not understood.

NTE is an evolutionarily conserved protein also found in *Drosophila*, where it is called Swiss-Cheese (SWS). This name is due to the formation of numerous vacuoles that develop in the nervous system of adult flies when SWS is lacking or mutated (Kretzschmar et al., 1997). While the brain appears to develop normally in these flies, vacuoles and

* Corresponding author.
E-mail address: kretzsch@ohsu.edu (D. Kretzschmar).
[1] Present address: School of Medicine, University of Colorado, 12,700 E. 19th Avenue, Aurora, CO 80045, United States of America.

https://doi.org/10.1016/j.nbd.2019.104520
Received 27 July 2018; Received in revised form 1 May 2019; Accepted 20 June 2019
Available online 22 June 2019
0969-9961/

neuronal cell death become evident around day 5 of adulthood and this increases with further aging. This is accompanied by progressive locomotion deficits and finally premature death (Kretzschmar et al., 1997). In addition to the neuronal degeneration, *sws* mutant flies show defects in the ensheathment of neurons by glia, followed by glial degeneration (Dutta et al., 2016). In agreement with its role in glia, SWS is expressed in glial cells, specifically ensheathing glia (Dutta et al., 2016), in addition to expression in all or most neurons (Muhlig-Versen et al., 2005). Similarly, NTE has been detected in Schwann cells in addition to neurons and it was shown to be upregulated in Schwann cells after neuronal injury (McFerrin et al., 2017). Confirming conserved roles of SWS and NTE, NTE can functionally replace SWS and prevent the neuronal and glial phenotypes in *sws* mutant flies (Muhlig-Versen et al., 2005).

Like NTE, SWS contains an esterase domain that mediates the phospholipase activity and *sws* mutant flies show an increase in PC and LPC (Muhlig-Versen et al., 2005; Kmoch et al., 2015). PC is a major component of all cell membranes and, like other phospholipids, it is mostly synthesized in the endoplasmic reticulum (ER) (Kienesberger et al., 2009; Lagace and Ridgway, 2013). Furthermore, substantial amounts of a cell's PC are localized in the ER, which forms a large membranous network within the cell, but also transfers and secretes lipids to other cellular compartments and to the extracellular environment. Therefore, it is not surprising that both, SWS and NTE are enriched in the ER and that a loss of SWS or NTE causes disruptions of the ER in flies and mice (Glynn et al., 1998; van Tienhoven et al., 2002; Akassoglou et al., 2004; Muhlig-Versen et al., 2005). The ER is also crucial to respond to stress situations by activating the unfolded protein response (UPR), which can be induced by the accumulation of unfolded or misfolded proteins in the ER (Hetz and Mollereau, 2014; Mei et al., 2013). When activated, the UPR signaling pathway inhibits protein translation, promotes protein degradation pathways, and increases the production of chaperones. In addition, it upregulates proteins required for lipid synthesis and ER function to deal with the increasing demand for the ER. While these initial responses are aimed at decreasing the stress and promoting cell survival, sustained activation of the UPR triggers apoptosis pathways and leads to cell death. Therefore, UPR responses can be protective or deleterious and both of these functions have been shown to play a role in a variety of neurodegenerative diseases (Hetz and Mollereau, 2014; Paschen and Mengesdorf, 2005; Roussel et al., 2013). ER stress responses can also be activated by changes in lipid composition by inhibiting the Sarco-Endoplasmic Reticulum Ca^{2+}-ATPase (SERCA), resulting in a decrease of ER Ca^{2+} stores and activation of the UPR (Fu et al., 2011; Paran et al., 2015). Overexpression of SERCA or the use of an agonists, can prevent these effects on the ER and also normalize lipid composition (Fu et al., 2011; Kang et al., 2016). Due to the increased levels of PC and LPC in the *sws* mutant and NTE knock-out mouse (Muhlig-Versen et al., 2005; Read et al., 2009), we therefore investigated whether SERCA inactivation and ER stress responses are activated in *sws* mutants and whether this has an effect on the degenerative and behavioral phenotypes.

2. Materials and methods

2.1. Drosophila stocks

The sws^1 allele has been described in (Kretzschmar et al., 1997). *Appl*-GAL4 was kindly provided by L. Torroja (Universidad Autonoma de Madrid, Spain), CaLexA by Jing W. Wan (University of California, San Diego), UAS-m-XBP1s by D. Rincon-Limas (University of Florida College of Medicine, Gainesville, FL), and *natalisin*-GAL4 by Y. Park (Kansas State University, KS). CantonS, *elav*-GAL4, UAS-XBP1-EGFP, UAS-SERCA, and the RNAi lines against IPLA2 (#36129) and LPCAT (#62918) were obtained from the Bloomington Stock Center. Flies were maintained on standard fly food (Caltech media) under a 12:12 h light:dark cycle. Stocks were maintained at 18 °C while crosses and aging flies were maintained at 25 °C. When analyzing flies from genetic crosses, control flies and sws^1 mutants flies to which these were compared, were outcrossed to wild type CantonS to ensure that effects were not due to background effects of the inbred lines. We only used male flies in our experiment because the *sws* gene is localized on the X-chromosome (Kretzschmar et al., 1997), and we can therefore obtain sws^1 hemizygous mutants in the first filial generation when performing crosses.

2.2. Western blots

Western Blots were performed as described in (Carmine-Simmen et al., 2009). Lysates of 3–4 heads were loaded on 10% SDS gels and blotted onto PVDF membranes. Primary antibodies used were anti-GRP78 1:2000 (StressMarq SPC-180D), anti-GFP 1:2000 (ThermoFisher Scientific A-11122), anti-SERCA 1:1000 (abcam 2A7-A1) and anti-GAPDH 1:333 (Santa Cruz G-9). Anti-Actin 1:200 (Hybridoma JLA20) developed by J. Lin was obtained from the Developmental Studies Hybridoma Bank, created by the NICHD of the NIH and maintained at The University of Iowa, Department of Biology, Iowa City, IA 52242. All antibodies were diluted in TBS-T supplemented with 5% milk powder and incubated overnight at 4 °C. Bands were visualized using horseradish peroxidase-conjugated secondary antibodies (Jackson ImmunoResearch) at 1:10,000 at room temperature for 1.5 h and SuperSignal West Pico or Femto chemiluminescent substrate (ThermoScientific). At least three replicates were performed. Statistical analysis was done using GraphPad Prism. The GRP78 westerns were analyzed with ANOVA and a Dunett's multiple comparison test. The CaLexA GFP western was analyzed with an unpaired two-tailed Student's *t*-test.

2.3. Reverse transcription (RT)-PCR

Total RNA was extracted from heads of adults aged to 7 days using Trizol (Life Technologies, Carlsbad, CA, USA) and cDNA synthesis was performed using SuperScript III (Life Technologies) and equal amounts of RNA. PCR with Q5 high-fidelity DNA polymerase (New England BioLabs, MA, USA) and primers flanking the unconventional splice site in *xbp1* messenger RNA (Xbp1_F GAACTGAAGCAGCAACAGCA and Xbp1_R GCCACAACTTTCCAGAGTGA) were used to amplify *xbp1* cDNA. After 30 cycles, equal volumes of PCR product were run on a 3% agarose gel and visualized with Ethidium bromide. The unspliced band was observed at 221 base pairs and the spliced variant was observed at 198 base pairs. Band intensity was measured using Fiji (Schindelin et al., 2012).

2.4. Negative geotaxis and phototaxis assays

For each genotype tested, 8–15 flies were placed into an empty vial and allowed to recover from CO_2 anesthetization for 2 h. The flies were then banged down to the bottom of the vial, allowed to ascend, and the number of flies that crossed 3 cm by 5 s was counted. The percentage of flies crossing the marker was calculated for each trial, averaged, and used for statistical comparisons. Statistical analysis was done using GraphPad Prism. When only two genotypes or treatments were compared, the data was analyzed with an unpaired two tailed Student's *t*-test. A one-way ANOVA was used to compare across multiple genotypes, and when a significant difference was found among the means, a multiple comparisons test was conducted comparing the means to sws^1 carrying only the *Appl*-GAL4 driver with a Dunnett's correction for multiple comparisons. Fast phototaxis assays were conducted in the dark using the countercurrent apparatus described by Benzer (1967) and a single light source. A detailed description of the experimental conditions can be found in Strauss and Heisenberg (1993). Flies were starved overnight, but had access to water and were tested the following morning. Five consecutive tests were performed in each experiment with a time allowance of 6 s to make a transition towards the

light and into the next vial. The short time renders the paradigm sensitive for walking speed. Flies were tested in groups of 5–10 flies. When using both, males and females were tested separately but combined to one value when they did not show significant differences. GraphPad Prism and one way Anova with post Dunett tests were used to determine significance when several experimental groups were compared.

2.5. Tissue sections and measurements of vacuoles

Paraffin sections for light microscopy were prepared and analyzed for vacuole formation as described in (Botella et al., 2003; Sunderhaus and Kretzschmar, 2016). Briefly, whole flies were fixed in Carnoy's fixative and dehydrated in an ethanol series followed by incubation in methyl benzoate before embedding in paraffin. Sections were cut at 7 μm and analyzed with a Zeiss Axioscope 2 microscope using the autofluorescence caused by the dispersed eye pigment. To quantify the vacuolization, we photographed sections without knowing the genotype at the level of the great commissure and numbered the pictures for a double-blind analysis. The area of vacuoles in the deutocerebral neuropil was then calculated in ImageJ as total pixel number, converted into μm^2, and the genotype/treatment determined. Statistical analyses were done using GraphPad Prism with an unpaired two tailed Student's *t*-test or one-way ANOVA and a Sidak's correction for multiple comparisons.

2.6. Immunohistochemistry

Brains were dissected in ice-cold PBS and transferred to 4% PFA in PBS. They were then fixed for 1 h at room temperature (RT) and washed three times with PBS/0.5% Triton (PBS-T) for 10 min each before blocking with 5% goat serum in PBS-T over night at 4 °C. Anti-GFP was used at 1:500 and rabbit anti-DmNTL4 ((Jiang et al., 2013a), kindly provided by Y-J. Kim, Gwangju Institute of Science and Technology, South Korea) at 1:1000 overnight at 4 °C. Brains were then washed three times, 20 min each at RT and the secondary antibody applied (anti-rabbit-GFP, Jackson ImmunoResearch) at 1:500 for 2–4 h at RT. Brains were washed three times for 20 min with PBS-T and mounted in Glycergel for confocal imaging. Confocal imaging was done using an Olympus FluoView 300 laser scanning confocal head mounted on an Olympus BX51 microscope.

2.7. Lipid analyses

Forty *Drosophila melanogaster* heads were collected and 5 μl of Lipidomix™ was added as an internal standard to each sample. Cold methyl tert-butyl ether:methanol:water was added and the heads pulverized using a ceramic bead blaster, centrifuged and the top layer was collected for UPLC-HDMS and UPLC-SWATH analyses. Samples were analyzed in duplicates in positive and negative ion modes. Acquired data was searched by Peakview's™ XIC Manager and LPC, PC and PE XIC (extracted ion chromatograms) lists were searched based on formula, accurate mass, isotope ratio and msms fragmentation. These experiments were conducted at the Mass Spectrometry Facility of the Oregon State University. Analyses of the lipid results was done with the help of M. Lasarev, a statistician at the Oregon Institute of Occupational Health Sciences. Totals for LPC, PC, and PE were each divided by 50,000 prior to analysis to improve scale. Technical duplicates from the same batch were summarized by taking the geometric mean of the two (scaled) totals. These geometric means served as the response in a two-way analysis between batch and genotype. The range of values across genotypes within any given batch differed by more than a factor of 5, suggesting a log scale being more appropriate for analysis. PC and PE were analyzed assuming a Gaussian distribution with log-link, while LPC was more appropriately modeled as a Gamma distribution, also with a log-link. The ratios between LPC:PE and PC:PE were also analyzed assuming Gaussian distribution with log-link. Three specific contrasts of interest (comparing SERCA and XBP1 each against sws^1 alone) were tested at the 0.017 level (Bonferroni-adjusted for three tests) for each response. For the comparisons of saturated and unsaturated fatty acids, levels were normalized to PE and values determined as fold change to the levels in sws^1. One way Anova with post Dunett tests was used to determine significance.

2.8. TUDCA treatment

Tauroursodeoxycholic acid was obtained from EMD Millipore (Cat #: 580549-5GM) and was added to regular *Drosophila* food at a final concentration of 15 mM (Debattisti et al., 2014.). Flies were kept on food with and without TUDCA after eclosion and transferred to a new vial after 7 days.

3. Results

3.1. Loss of SWS results in induction of the unfolded protein response

As mentioned above, changes in lipid levels have been described after the loss of SWS/NTE in flies and mice and such changes could activate the ER stress response. We therefore investigated whether *sws* mutant flies show an activation of ER stress responses, possibly as a means to protect affected neurons. sws^1 mutants show age-dependent neuronal degeneration with the first signs becoming visible after 5–6 days post eclosion (Kretzschmar et al., 1997). We therefore collected control flies and sws^1 flies at 7 days of age when the neurons are already affected but the degeneration is not so severe that it affects overall protein levels. To detect an activation of ER stress responses, fly heads were collected and Western blots performed to determine the levels of GRP78/BiP, a chaperone in the ER whose transcription is activated during ER stress in an attempt to protect the cell. As shown in Fig. 1A, GRP78/BiP levels were significantly increased in the sws^1 mutants. Quantifying this effect (Fig. 1B) showed that the loss of SWS caused a significant rise in GRP78/BiP levels, suggesting that ER stress responses are activated in sws^1 to prevent cellular damage. Next, we confirmed that the induction of stress responses is in fact due to the mutation by reintroducing SWS in *sws* flies. Expressing SWS pan-neuronally with the *Appl*-GAL4 driver significantly reduced the levels of GRP78/BiP in *sws* to the levels seen in controls, confirming that activation of the ER stress response was due to the loss of SWS (Fig. 1A, B).

Protective ER stress responses are initiated by the release of GRP78/BiP from the signaling molecules Activating Transcription Factor 6 (ATF6) and Inositol-Requiring Enzyme 1 (IRE1) (Wang et al., 2009). In contrast, activation of the stress sensor PERK promotes apoptosis by activating caspases. Whereas ATF6 directly regulates transcription, activated IRE1 acts as an endoribonuclease that cuts an intron from the mRNA of the X-Box Binding Protein (XPB1) (Dunys et al., 2014; Kim et al., 2006). This results in the translation of the XBP1 transcription factor, which can then translocate to the nucleus and upregulate genes associated with lipogenesis, ER associated protein degradation, chaperones like GRP78/BiP, and ER remodeling proteins to promote cell survival. We therefore analyzed the splicing pattern of XBP1 as another means to show that a protective ER stress response is induced in *sws*. As shown in Fig. 1C, D, the spliced mRNA of XBP1, which is 26 bp smaller than the unspliced form, is about four fold increased in 7d old sws^1 mutants, while the levels of the unspliced form are unchanged. This provides additional support that ER stress is activated in *sws* mutants and it suggests that the initiation occurs via the IRE1 pathway.

3.2. Increasing XBP1 levels ameliorates sws-associated behavioral and neurodegenerative phenotypes

As discussed above, the splicing and activation of XBP1 is a response of the ER aimed at preventing cellular damage. We therefore tested whether additional expression of XBP1 could ameliorate the

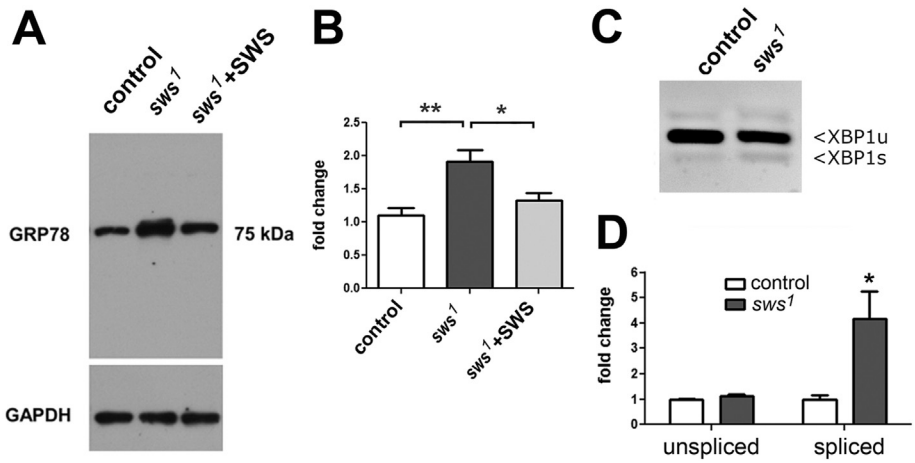

Fig. 1. Loss of SWS activates ER stress responses. A) Western blot using head homogenates and anti-GRP78. Higher levels of GRP78 are detectable in *sws*^{1} flies (*sws*^{1}*Appl*-GAL4*)* compared to controls (only *Appl*-GAL4). Expressing SWS pan-neuronally in *sws*^{1} flies (*sws*^{1}*Appl*-GAL4 > UAS-SWS) reduces GRP levels. Anti-GAPDH is used as loading control. B) Quantifying GRP78 protein levels confirms a significant increase in *sws*^{1} compared to the controls. Expressing SWS in neurons in *sws*^{1} mutants significantly reduces GRP78 levels compared to *sws*^{1} while they are not significantly different from the controls. Data represent the mean and SEM of 4 independent Western blots. Flies were 4-6d old males. C) Image of PCR fragments showing increased splicing of XBP1 in *sws*^{1} compared to controls. XBP1u = unspliced, XBP1s = spliced. D) Quantifying the levels of unspliced XBP1 reveals no significant difference while the levels of spliced XBP1 is significantly higher in *sws*^{1}. Data represent the mean and SEM of 3 independent Western blots. Flies were 7d old. * $p < 0.05$, ** $p < 0.01$.

phenotypes caused by the loss of SWS. For this experiment, we induced expression of *Drosophila* XBP1 (tagged with EGFP) pan-neuronally, again using *Appl*-GAL4. To detect *sws*^{1}-associated locomotor defects we used negative geotaxis assays which revealed a robust phenotype in 7 day old mutants (Fig. 2A) and this reduction in locomotion is significantly improved when we expressed XBP1 (Fig. 2A). Because this XBP1 construct contains the intron, the resulting mRNA must be spliced to get translated, further supporting an activation of the IRE1/XBP1 pathway in *sws*^{1}. We confirmed a protective effect of XBP1 by expressing murine XBP1, using a construct without the intron (UAS-m-XBP1-s). Although not as effective as the fly version, m-XBP1-s also suppressed the deficits in the negative geotaxis tests (Fig. 2A). To test whether XBP1 can suppress the neurodegeneration in *sws*^{1}, we aged the flies to 14d, an age when degeneration is easily detected by the formation of vacuoles (Fig. 2C). Quantifying the area of vacuoles in the deutocerebral neuropil showed that the neurodegeneration seen in the *sws*^{1} mutant was reduced when expressing XBP1 or m-XBP1-s (Fig. 2B, D, E). This shows that XBP1 expression and downstream activation of cytoprotective mechanisms can ameliorate the behavioral and neurodegenerative effects caused by the loss of SWS. Analyzing the levels of GRP78/BiP in 7d old *sws*^{1} flies overexpressing XBP1, we found a decrease but this did not reach significance (Supplementary Fig. 1). However, when analyzing 14 d old flies, the levels of GRP78/BiP were reduce to the levels in controls (Fig. 2F), suggesting that the increased levels of XBP1 attenuates the ER stress response.

3.3. Expression of Sarco-endoplasmic reticulum Ca2+ ATPase alleviates *sws*^{1} deficits

Sarco-Endoplasmic Reticulum Ca^{2+} ATPase (SERCA) is the pump that balances calcium between the ER and the cytosol by pumping Ca^{2+} into the ER to ensure proper protein folding and chaperone function (Hojmann Larsen et al., 2001). In neurons, a healthy ER is vital for the transport of materials within axons and to act as a Ca^{2+} pool to ensure folding of proteins and firing of action potentials along the axon (Verkhratsky, 2005). The ER is also a major storage site of Ca^{2+} to prevent the initiation of the apoptotic pathways that are activated when the levels of Ca^{2+} in the cytosol are too high (Verkhratsky, 2005). It has been described that changes in lipid homeostasis, specifically an elevation of PC, in the ER results in the inhibition of SERCA, thereby affecting Ca^{2+} homeostasis and contributing to ER stress (Fu et al., 2011). Therefore, the rise in PC and LPC levels in *sws* mutants could affect SERCA and as a consequence ER/cytosol Ca^{2+} balance. To determine effects of *sws* on SERCA, we first performed Western blots using an antibody against vertebrate SERCA and 7d old flies. To identify the correct band, we included flies overexpressing SERCA. Comparing *sws*^{1} with controls showed that SERCA levels (arrowhead, Fig. 3A) were reduced in the *sws*^{1} mutant. If the reduction in SERCA plays a role in the pathogenic mechanisms in *sws*, additional expression of SERCA should also suppress the phenotypes caused by the loss of SWS. We therefore performed negative geotaxis assays with *sws*^{1} flies expressing SERCA in neurons via *Appl*-GAL4. As shown in Fig. 3B, this resulted in a significant improvement of the locomotor deficits of 7 day old *sws*^{1} mutants. In addition, SERCA expression decreased the neurodegeneration in 14 day old mutants, as quantified by area of vacuoles (Fig. 3C–E). This provides further supports that changes in SERCA and Ca^{2+} homeostasis contribute to the mutant phenotypes that develop in *sws*^{1}. To verify changes in Ca^{2+}, we used the CaLexA system to express the LexA/NFAT transcription factor (Masuyama et al., 2012) pan-neuronally using *elav*-GAL4. When cytosolic Ca^{2+} levels rise, LexA/NFAT is dephosphorylated and translocates from the cytosol to the nucleus (Supplementary Fig. 2). There it activates the LexA operon, causing the expression of GFP. Using an antibody to detect GFP, we found a significant increase in GFP levels in *sws*^{1} versus the control, suggesting increased Ca^{2+} levels in the cytosol of *sws* mutants (Fig. 4A, B). This was confirmed by expressing LexA/NFAT with *Natalisin*-GAL4 (Jiang et al., 2013b) and performing immunohistochemistry on brain whole-mounts. Natalisin is expressed in four pairs of large neurons (one of them is shown in Fig. 4C) and we previously showed that these neurons express high levels of SWS (Bettencourt da Cruz et al., 2008; Cassar et al., 2018). As expected, we observed an increase of GFP in the cytosol of these neurons in *sws*^{1} compared to the control (Fig. 4D, E). These experiments confirm changes in Ca^{2+} balance in *sws*^{1}, whereby the decrease in SERCA and the resulting increase in cytosolic Ca^{2+} may cause the apoptotic neuronal cell death that we previously described in aged *sws*^{1} (Kretzschmar et al., 1997). Due determine whether SERCA expression has an effect on the ER-stress responses mediated by the induction of GRP78/BiP, we again used Western blot analyses but did not detect a significant change in GRP78/BiP levels between *sws*^{1} flies and *sws*^{1} flies expressing additional SERCA (Supplementary Fig. 1).

3.4. Lipid homeostasis is improved when XBP1 or SERCA is expressed

The results described above show that additional expression of XBP1 ameliorates *sws*-associated phenotypes. When activated, XBP1 can regulate enzymes involved in lipid synthesis (Han and Kaufman, 2016; Lagace and Ridgway, 2013) and we therefore tested whether its protective function may be due to improving lipid composition in *sws*^{1}.

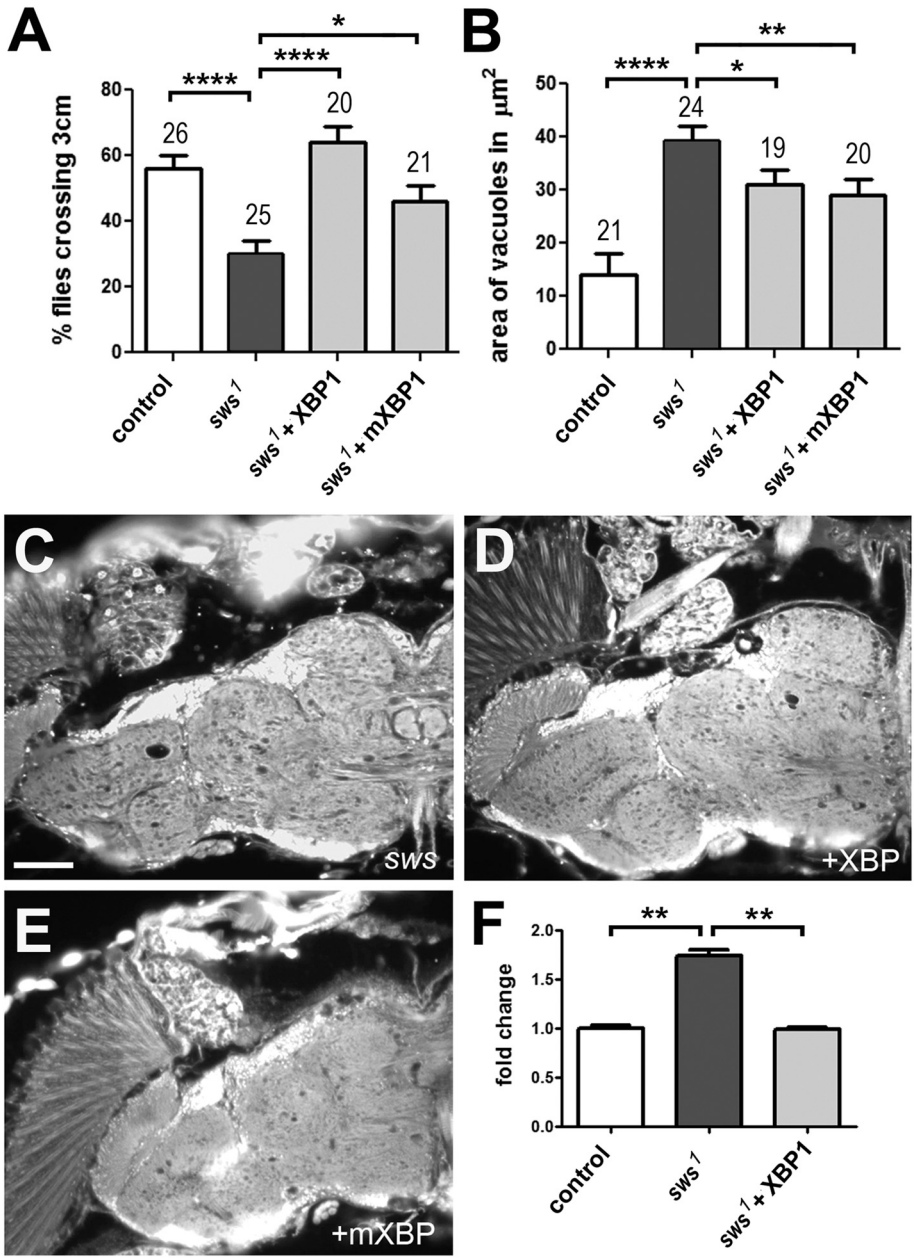

Fig. 2. XBP1 expression rescues *sws*[1]. A) Expression of fly XBP1-EGFP (XBP1) or mouse XBP (mXBP1) with *Appl*-GAL4 suppresses the locomotor deficits observed in *sws*[1] (*sws*[1]*Appl*-GAL4) when 7d old. B) Quantifying neurodegeneration at 14d of age reveals that expression of XBP1 or m-XBP1 suppresses the *sws*[1]-associated neurodegeneration. Data represent the mean and SEM. The number of independent trials of 8 or more flies used in A or heads used in B is indicated above the bar. C) Head section from a 14d old *sws*[1] fly (*sws*[1]*Appl*-GAL4) shows the formation of vacuoles in the brain. The formation of vacuoles is suppressed when either fly (D; *sws*[1]Appl-GAL4 > UAS-XBP1-EGFP) or mXBP1 (E; *sws*[1]Appl-GAL4 > UAS-mXBP1) is expressed. Scale bar for C-E = 25 µm. F) GRP78 levels are decreased when expressing XBP1 in *sws*[1] (*sws*[1]Appl-GAL4 > UAS-XBP1-EGFP) compared to *sws*[1]. Data represent the mean and SEM of 3 independent Western blots. Flies were 14d old. *$p < 0.05$, **$p < 0.01$, ****$p < 0.0001$.

It was previously described that loss of SWS/NTE results in a rise in PC and LPC levels in flies and mice (Kmoch et al., 2015; Muhlig-Versen et al., 2005; Read et al., 2009) and using head extracts from control flies and *sws*[1] confirmed these results (Fig. 5). PC and LPC levels were normalized to phosphatidylethanolamine, which we previously showed not to be affected in *sws* (Muhlig-Versen et al., 2005). As expected, expression of XBP1 was able to significantly reduce the LPC/PE ratio (Fig. 5A) however, it did not affect the PC/PE ratio (Fig. 5B). More surprisingly, SERCA expression had the same effect and also reduced LPC levels but not PC levels (Fig. 5A, B). Although XBP1 and SERCA expression only reduces LPC levels they both significantly suppressed *sws*-related phenotypes, indicating that the increase in LPC levels may be more pathogenic than the increase in PC.

It has been shown that LPC is the preferred substrate of SWS/NTE (Quistad et al., 2003; van Tienhoven et al., 2002) and therefore an increase in LPC levels is expected after the loss of SWS/NTE. However, in both flies and mice PC levels are also increased (Kmoch et al., 2015; Read et al., 2009). PC can be generated from LPC by lysophosphatidylcholine acyltransferases (LPCAT), which preferentially incorporates polyunsaturated fatty acids (Lagace and Ridgway, 2013; Parks and Gebre, 1997). We therefore determined the levels of saturated, monounsaturated, and polyunsaturated fatty acids in *sws*[1] versus controls. Whereas the levels of saturated PCs were not different in *sws*[1] head extracts versus controls (Fig. 6A), the levels of monounsaturated and even more so polyunsaturated PCs were significantly increased in *sws*[1] (Fig. 6B, C). This indicates that the increase in PC levels in the mutant could be a consequence of the increased levels of LPC and increased LPCAT activity. Determining the changes in LPC species, we found that all types were significantly increased in *sws*[1] (Fig. 6D-F). As expected form the results in Fig. 5, showing no effects of XBP1 and SERCA overexpression on overall PC levels, neither had an effect on the different types of fatty acids. However, although both decreased overall LPCs levels, SERCA decreased the levels of saturated LPCs, whereas XBP1 decreased the levels of monounsaturated and polyunsaturated LPCs.

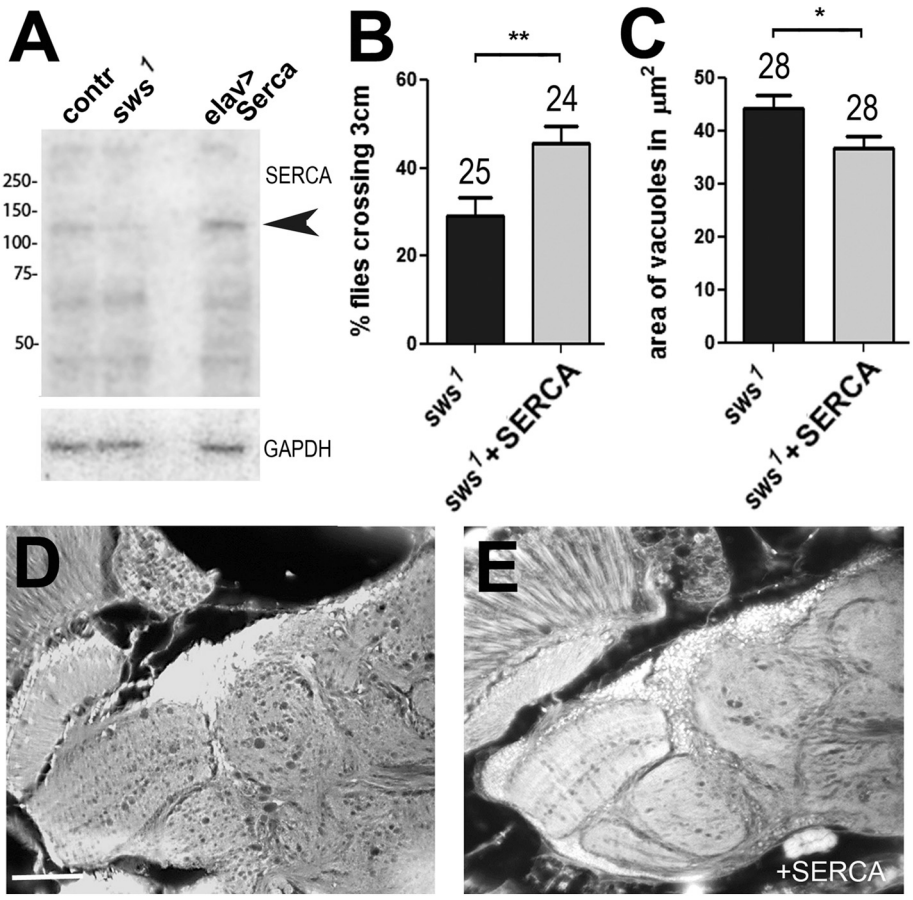

Fig. 3. SERCA expression rescues *sws*[1]. A) A Western blot shows a reduction in SERCA levels in *sws*[1]. The identity of the band representing SERCA (arrowhead) is confirmed by overexpressing SERCA with *elav*-GAL4. Anti-GAPDH is used as loading control. Flies were 7d old. B) SERCA expression (*sws*[1]Appl-GAL4 > UAS-SERCA) significantly suppresses the negative geotaxis deficits in 7d old *sws*[1]. C) Quantifying the area of vacuoles shows that expression of SERCA also significantly rescues the neurodegeneration of *sws*[1] at 14d. Data represent the mean and SEM. The number of independent trials of 8 or more flies used in B or heads used in C is indicated above the bar. *p < 0.05, **p < 0.01. D) Head section of a 14d old *sws*[1] fly (*sws*[1]Appl-GAL4) E) Head section from a 14d old *sws*[1] fly expressing additional SERCA (*sws*[1]Appl-GAL4 > UAS-SERCA). Scale bar for D, E = 25 µm.

3.5. sws-like phenotypes and ER stress in LPCAT and iPLA2-VIA knockdowns

The findings presented above provide strong evidence that changes in lipid composition and especially an increase in LPC are inducing ER stress and play an important role in inducing the phenotypes in *sws*[1]. To obtain further support for this, we manipulated other proteins involved in lipid homeostasis. As mentioned above, LPC can be converted into PC by the acetyltransferase LPCAT thereby reducing LPC levels. We therefore tested whether a knockdown of LPCAT can induce ER stress and lead to similar phenotypes as observed in *sws*. Measuring GRP78/BiP levels in the panneuronal *elav*-GAL4 induced knockdown showed a significant increase in GRP78/BiP compared to the wild type control when analyzing 7d old flies (Fig. 7A). In addition, LPCAT knockdown flies showed locomotion defects when 14d old (Fig. 7B) and they revealed some neurodegeneration at 30d (arrows, Fig. 7C). More dramatic effects were detected when knocking down iPLA2-VIA, a member of the calcium-independent phospholipases that catalyze the hydrolysis of PCs to LPCs and affect the function of various organelles, including the ER and mitochondria (Ramanadham et al., 2015). PLA2G6, the human homologue of fly iPLA2-VIA, has been connected to several neurodegenerative diseases and flies lacking iPLA2 show a severe degenerative phenotype when aged and defects in negative geotaxis (Kinghorn et al., 2015). As shown in Fig. 7D, we confirmed the neurodegeneration in 30d old iPLA2-VIA knockdown flies and we also detected a strong reduction in performance in the phototaxis test at 14d (Fig. 7B). This is another assay to analyze locomotion deficits and *sws*[1] is also performing poorly in this test (Fig. 7B). Furthermore,uPLA2-VIA knockdown flies showed an increase in GRP78/BiP levels when 7d old (Fig. 7A), showing that other genetic manipulations that interfere with PC/LPC homeostasis induce ER stress responses similar to *sws*[1].

3.6. Tauroursodeoxycholic acid treatment alleviates sws[1] *phenotypes*

Tauroursodeoxycholic Acid (TUDCA) is a bile salt that has been shown to reduce ER stress associated with elevated glucose levels in diabetes and it is also a potent inhibitor of apoptosis by stabilizing mitochondrial membranes to prevent the release of cytochrome C, Bax translocation and caspase 3 activation (Rodrigues et al., 2003; Schoemaker et al., 2004; Vang et al., 2014). Due to this anti-apoptotic activity, TUDCA has been tested as a possible treatment for several neurodegenerative diseases, including Alzheimer's disease, Parkinson's disease, and amyotrophic lateral sclerosis (Vang et al., 2014). TUDCA treatment has also been shown to suppress phenotypes in *Drosophila* models of neurodegeneration (Debattisti et al., 2014; Tsuda et al., 2017). We therefore tested whether it can slo ameliorate *sws*[1]-associated phenotypes. For this experiment, we reared and aged flies on food that contained 15 mM TUDCA, a concentration previously shown to be effective in *Drosophila* (Debattisti et al., 2014). As shown in Fig. 8A, treated 7d old *sws*[1] flies performed significantly better in the negative geotaxis test than age-matched control *sws*[1] flies kept on food without TUDCA. Analyzing neurodegeneration at 14 days of age also showed an improvement in treated *sws*[1] flies (Fig. 8B-D). These results show that treatment with TUDCA is able to decrease both, the degenerative and behavioral phenotype of *sws*[1]. We also measured GRP78/BiP levels in these flies but did not detect a significant effect by TUDCA treatment (Supplementary Fig. 3), suggesting that the treatment does not promote protective ER stress responses but may reduce apoptotic death in the mutant.

4. Discussion

Loss of SWS/NTE function causes locomotion deficits, neuronal degeneration, and a shortened life span. It has also been shown that

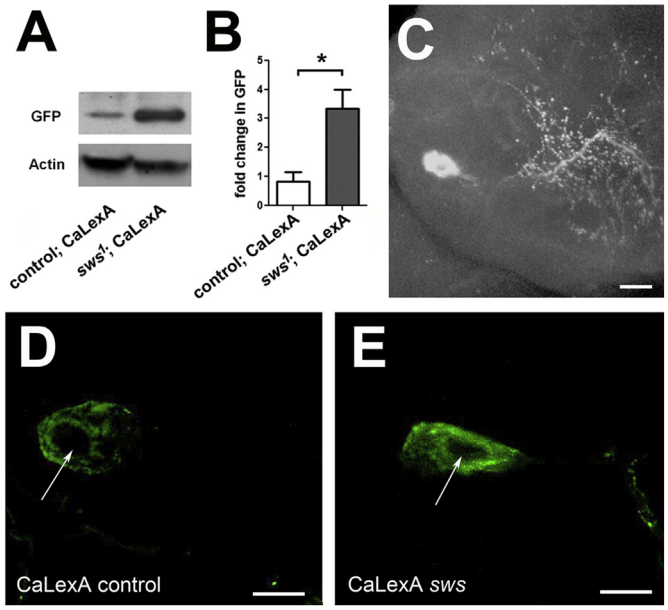

Fig. 4. Higher levels of Ca^{2+}, as detected by increased GFP using the CaLexA system, are detected in *sws*[1]. A) Western blot using anti-GFP and head homogenates shows increased levels of GFP in *sws*[1]. GFP is expressed by inducing CaLexA pan-neuronally with *elav*-GAL4. Actin is used as a loading control. B) Quantification of the GFP levels showing increased levels of GFP, indicating higher levels of cytosolic Ca^{2+} levels in *sws*[1]. Data represent the mean and SEM from 3 independent Western blots. *p < 0.05. C) Image showing one of the large Natalisin-positive neurons. C, D) Inducing CaLexA with Natalisn-GAL4 results in low GFP levels in the cytosol of this large neuron in the control (C) while GFP levels are increased in *sws*[1] (D). The arrows point to the nucleus. Scale bar in C = 10 μm, in D, E = 5 μm.

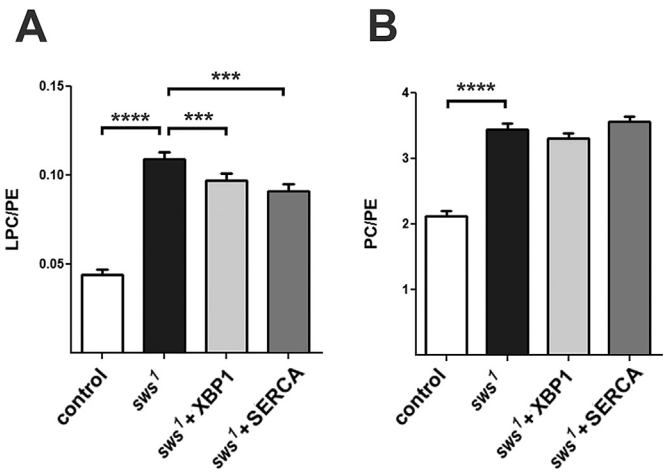

Fig. 5. LPC levels are reduced by expression of SERCA or XBP1. A) Pan-neuronal expression of SERCA or XBP1 (*sws*[1]Appl-GAL4 > UAS-SERCA and *sws*[1]Appl-GAL4 > UAS-XBP1-EGFP) significantly reduce the LPC/PE ratio in *sws*[1]. B) Neither expression of SERCA nor XBP1 reduces the PC/PE ratio in *sws*[1]. Data represent the mean and 95% intervals of 3 independent batches. Flies were 3-5d old males. ***p < 0.001, ****p < 0.0001.

SWS/NTE acts as a phospholipase that can deacetylate lysophosphatidylcholine (LPC) to produce glycerophosphocholine (Quistad et al., 2003; van Tienhoven et al., 2002) and that the loss of SWS/NTE leads to an increase in PC and LPC (Kmoch et al., 2015; Muhlig-Versen et al., 2005; Read et al., 2009). We therefore investigated whether and how this change in lipid homeostasis may lead to the behavioral and degenerative phenotypes in the mutants. PC is synthesized and abundant in the ER and it is crucial for the membrane expansions that occur during ER stress, therefore its production is increased during ER stress (Lagace and Ridgway, 2013; Mei et al., 2013; Roussel et al., 2013; Hetz and Mollereau, 2014). However, an increase in PC can also activate ER-stress responses as shown in the context of obesity and in a mouse model of muscular dystrophy (Fu et al., 2011; Paran et al., 2015), suggesting that the lipid content in the ER has to be tightly regulated. ER stress activates a complex signaling network that first promotes protective mechanism that include increasing lipid synthesis and producing chaperones like GRP78/BiP (Jiang et al., 2015; Wang et al., 2009; Wu et al., 2015). This occurs via transcriptional activation, either directly via ATF6 or indirectly via the splicing of XBP1. Our results that GRP78/BiP levels and XBP1 splicing is increased in *sws*[1] shows that protective ER stress responses are initiated in the mutant in an attempt to prevent cellular damage. Consequently, expressing additional XBP1 ameliorated the behavioral and neurodegenerative phenotypes of *sws*[1], and it reduced the increase in lipids, though this only reached significance for LPC. Although XBP1 has been considered a lipogenic factor, findings in liver have also demonstrated anti-lipogenic effects (Herrema et al., 2016) and the reduction in LPC therefore suggests that in the case of *sws*[1] XBP1 has anti-lipogenic functions. In addition, as seen by the reduction in GRP78/BiP, it terminated further activation of these transcriptional responses because GRP78/BiP not only acts as a chaperone but it also binds and inactivates the ER stress receptors, thereby acting in a negative feedback loop (Adams et al., 2019; Hetz and Mollereau, 2014).

An increase in ER lipid composition can also affect SERCA and therefore Ca^{2+} homeostasis. In obesity and muscular dystrophy mouse models, the increase in PC/PE ration has been shown to inhibit SERCA and calcium transport into the ER (Fu et al., 2011; Paran et al., 2015). Similarly, *sws*[1] mutant flies show on increase in cytosolic Ca^{2+}, which suggests reduced transport of Ca^{2+} into the ER, and a reduction in SERCA levels. That this contributes to the pathogenicity in *sws* is shown by our results that expression of SERCA also suppressed the locomotor deficit and neurodegeneration associated with *sws*[1]. Although the protective effect of SERCA on neuronal survival could be due to reducing cytosolic Ca^{2+} and thereby apoptosis (Pinton et al., 2008), SERCA expression also reduced LPC levels in *sws*[1]. Many enzymes depend on high Ca^{2+} levels, including phospholipases (Ritz et al., 1980), suggesting that an activation of other phospholipases could reduce LPC levels. Alternatively, SERCA promotes the chaperone function of GRP78/BiP, which is activated by Ca^{2+} (Carreras-Sureda et al., 2018), and therefore its release from IRE-1. Consequently, IRE-1 can cleave and activate XBP1, which then decreases the LPC/PE ratio. However, we think this is less likely because we should then also detect effects on GRP78/BiP levels when expressing SERCA but we did not. We also found that XBP1 and SERCA affected lipid levels differently. Although both reduced LPCs, SERCA expression decreased the levels of saturated LPCs while XBP1 expression reduced unsaturated LPCs, further supporting that they might act via different mechanisms on LPC levels.

sws[1] mutants show an increase in both, PC and LPC levels and although SERCA and XBP1 only reduce the LPC/PE ratio, they significantly suppress the behavioral and degenerative phenotype. This suggests that the pathology may be due to the elevated levels of LPC rather than PC. The LPC concentration in membranes is normally quite low but increased levels of LPC and LPA, which is produced from LPC, have been connected with a variety of diseases, including heart failure, atherosclerosis, diabetes, and most notably demyelination and neuropathic pain (Drzazga et al., 2014; Fuchs and Schiller, 2009; Velasco et al., 2017; Wang and Dennis, 1999). *Drosophila* does not produce myelin but glial cells in the fly nervous system do surround axons with a glial sheath and we previously showed that these sheaths are disrupted and incomplete in the *sws* mutant (Dutta et al., 2016). Furthermore, we showed that a glial specific knock-out of NTE in mice caused incomplete glial wrapping of Remak bundles by non-myelinating Schwann cells in the sciatic nerve (McFerrin et al., 2017). That elevated LPC levels may play a role in these glial defects is suggested by the

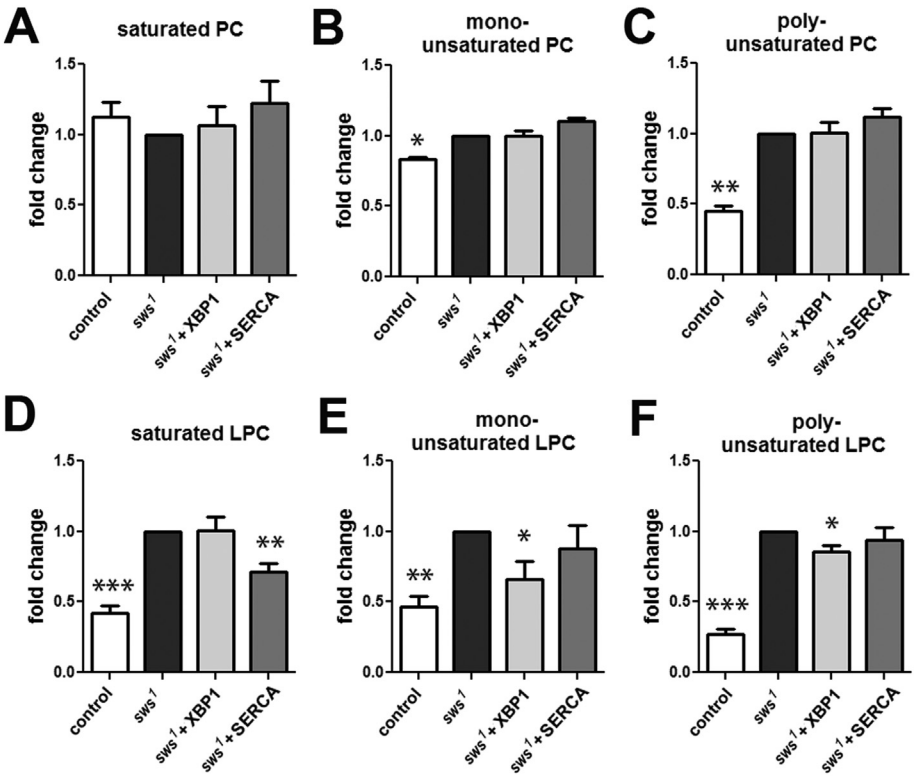

Fig. 6. XBP1 and SERCA have different effects on LPCs. A-C) The levels of saturated PCs are not significantly different in *sws*[1] head extracts compared to controls (A) whereas the levels of monounsaturated (B) and polyunsaturated PC (C) species are significantly increased in *sws*[1]. Additional expression of SERCA or XBP1 with *Appl*-GAL4 in *sws*[1] did not have an effect on any PC species. D-E) Both, saturated and unsaturated LPCs were reduced in *sws*[1] head extracts compared to controls. Additional expression of SERCA reduces the levels of saturated LPCs in *sws*[1] (D) but does not affect unsaturated LPCs (E, F). In contrast, expression of XBP1 in *sws*[1] has no effect on saturated LPCs but reduces the levels of unsaturated LPCs (E, F). 3 independent measurements were used and the mean and SEM is shown. Flies were 3-5d old males. *p < 0.05, **p < 0.01, ***p < 0.001.

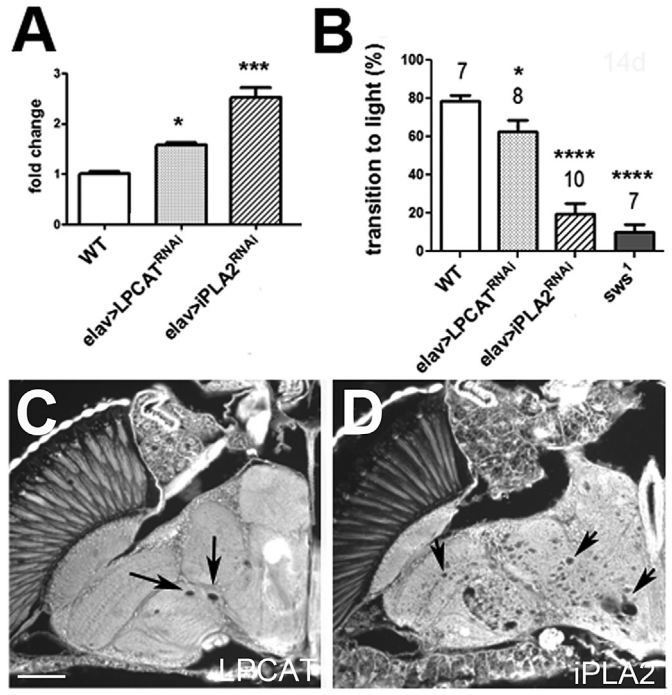

Fig. 7. ER stress and *sws*-like phenotypes in the LPCAT and iPLA2-VIA knockdowns. A) GRP78 levels are increased when LPCAT or iPLA2-VIA is knocked down in all neurons using *elav*-GAL4. Flies were 7d old. B) These flies also show deficits in locomotion in fast phototaxis assays when 14d old, as do 14d old *sws*[1] flies. Data represent the mean and SEM. 3 independent Western blots were analyzed in A and the number of independent trials of 8 or more flies is indicated in B. *p < 0.05, ****p < 0.0001. C) Head sections of a 30d old *elav*-GAL4 > UAS-LPCAT^{RNAi} fly shows a few vacuoles (arrows). D) Head sections of a 30d old *elav*-GAL4 > UAS-iPLA2-VIA^{RNAi} fly shows severe degeneration in these flies. Scale bar for C, D = 25 μm.

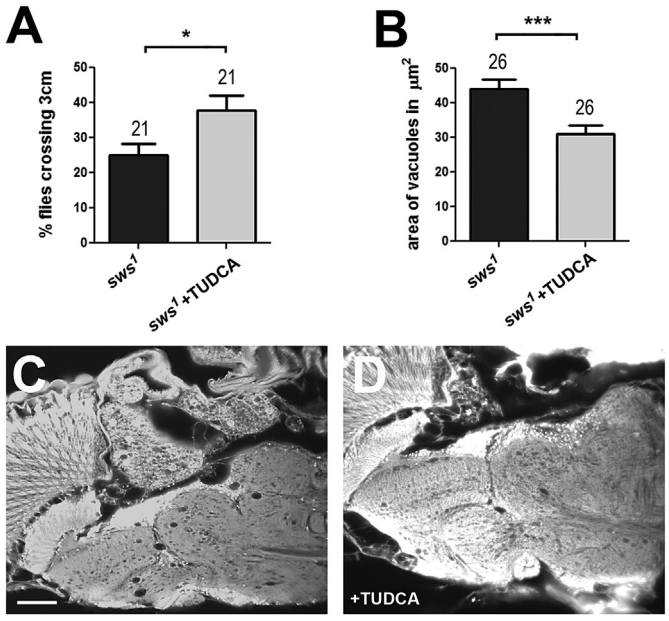

Fig. 8. Rearing flies on TUDCA treated food rescues *sws*[1]. A) Treating flies with TUDCA significantly rescues *sws*[1] negative geotaxis deficits at 7d. B) Quantifying the neurodegeneration also shows that TUDCA treatment significantly rescues this *sws*[1] phenotype at 14d. C) Head sections of a 14d old *sws*[1] fly reared on regular food. D) Head section of a 14d old *sws*[1] fly reared food with 15 mM TUDCA. Scale bar for C, D = 25 μm.

finding that a wild type form of SWS can restore the glial defects when expressed in glia in *sws* mutants, while a variant with a mutation in the active site of the lipase domain cannot (Dutta et al., 2016). However, lipid homeostasis is also crucial for the health and survival of neurons (as well as cell types outside the brain). Changes in lipid composition affects synaptic transmission by regulating vesicle fusion and endocytosis (Lauwers et al., 2016). Lipid composition controls the

thickness, fluidity, and curvature of membranes whereby incorporation of the cone-shaped structure of LPC induces more curvature than the cylinder-shaped PC, thereby affecting synaptic vesicle release (Lauwers et al., 2016). Such synaptic changes, due to the elevated LPC/PE levels and the altered membrane composition, could underlie the locomotion deficits in *sws* that are detectable before overt neuronal death occurs. Furthermore, lipid signaling plays an important role in inducing cell death. LPC has been shown to promote apoptosis by increasing the pro-apoptotic proteins Bax and cleaved caspase-3 (Chang et al., 2017; Kakisaka et al., 2012; Lin and Ye, 2003; Wang et al., 2016). Another effect of the elevated levels of LPC could therefore be that it promotes the apoptotic cell death we detected in *sws* mutants (Kretzschmar et al., 1997). Therefore, a reduction in the LPC/PE ratio, as detected after expression of SERCA and XBP1, may be sufficient to ameliorate the behavioral and degenerative phenotypes in the mutant. As mentioned above, the increase in PC in sws^1 could be a secondary effect due to the synthesis of more PC from the increased LPC by LPCAT (Lagace and Ridgway, 2013; Parks and Gebre, 1997). The crucial role of LPC in causing locomotion and neurodegenerative effects is further supported by our results that the knockdown of two other enzymes that reduce LPC levels, LPCAT and iPLA2-VIA, show similar phenotype as *sws*. They also increase GRP78/BiP levels, suggesting that LPC may be the key factor in inducing ER stress responses.

Lastly, we found that TUDCA treatment can ameliorate *sws*-associated phenotypes. TUDCA has been connected to ER stress responses by findings that it can attenuate ER stress-induced apoptosis and specifically the activation of Bax by preventing the release of Ca^{2+} from mitochondria (Vang et al., 2014). In agreement with this protective function, TUDCA treatment ameliorated the locomotion and degenerative phenotypes of *sws*, while it did not change GRP78/BiP levels.

In summary, our results suggest that the loss of SWS and its effect on PC/LPC levels leads to the activation of ER stress responses, SERCA inhibition and Ca^{2+} imbalance. Promoting protective ER responses or increasing SERCA activity protected against the deleterious effects and also reduced LPC levels, although this seems to occur by different mechanisms. Furthermore, TUDCA treatment ameliorated the locomotion and degenerative phenotypes associated with *sws*. TUDCA has been approved for treatment of biliary cirrhosis and is investigated as a therapeutic for patients with neurodegenerative diseases and our results suggest that it may also provide a treatment for NTE-related diseases.

Declaration of Competing Interests

None.

Acknowledgments

We thank Drs. L. Torroja, J. W. Wan, and D. Rincon-Limas for providing fly stocks and Y-J. Kim for providing antibodies. This work was supported by a grant from the National Institute of Health (NS047663) to D.K. and fellowship to E.S. from a training grant from the National Institute of Health (5T32AG023477).

Appendix A. Supplementary data

Supplementary data to this article can be found online at https://doi.org/10.1016/j.nbd.2019.104520.

References

Adams, C.J., et al., 2019. Structure and molecular mechanism of ER stress signaling by the unfolded protein response signal activator IRE1. Front. Mol. Biosci. 6, 11.
Akassoglou, K., et al., 2004. Brain-specific deletion of neuropathy target esterase/swisscheese results in neurodegeneration. Proc. Natl. Acad. Sci. U. S. A. 101, 5075–5080.
Benzer, S., 1967. Behavioral mutants of Drosophila isolated by countercurrent distribution. Proc. Natl. Acad. Sci. U. S. A. 58, 1112–1119.
Bettencourt da Cruz, A., et al., 2008. Swiss cheese, a protein involved in progressive neurodegeneration, acts as a noncanonical regulatory subunit for PKA-C3. J. Neurosci. 28, 10885–10892.
Botella, J.A., et al., 2003. Deregulation of the Egfr/Ras signaling pathway induces age-related brain degeneration in the Drosophila mutant vap. Mol. Biol. Cell 14, 241–250.
Carreras-Sureda, A., et al., 2018. Calcium signaling at the endoplasmic reticulum: fine-tuning stress responses. Cell Calcium 70, 24–31.
Carmine-Simmen, K., et al., 2009. Neurotoxic effects induced by the Drosophila amyloid-beta peptide suggest a conserved toxic function. Neurobiol Dis 33, 274–281.
Cassar, M., et al., 2018. The PKA-C3 catalytic subunit is required in two pairs of interneurons for successful mating of Drosophila. Sci. Rep. 8, 2458.
Chang, M.-C., et al., 2017. Lysophosphatidylcholine induces cytotoxicity/apoptosis and IL-8 production of human endothelial cells: related mechanisms. Oncotarget 8, 106177–106189.
Debattisti, V., et al., 2014. Reduction of endoplasmic reticulum stress attenuates the defects caused by Drosophila mitofusin depletion. J. Cell Biol. 204, 303–312.
Deik, A., et al., 2014. Compound heterozygous PNPLA6 mutations cause Boucher-Neuhauser syndrome with late-onset ataxia. J. Neurol. 261, 2411–2423.
Drzazga, A., et al., 2014. Lysophosphatidylcholine and lysophosphatidylinosiol–novel promissing signaling molecules and their possible therapeutic activity. Acta Pol. Pharm. 71, 887–899.
Dunys, J., et al., 2014. The transcription factor X-box binding protein-1 in neurodegenerative diseases. Mol. Neurodegener. 9, 35.
Dutta, S., et al., 2016. Glial expression of Swiss cheese (SWS), the Drosophila orthologue of neuropathy target esterase (NTE), is required for neuronal ensheathment and function. Dis. Model. Mech. 9, 283–294.
Fu, S., et al., 2011. Aberrant lipid metabolism disrupts calcium homeostasis causing liver endoplasmic reticulum stress in obesity. Nature. 473, 528.
Fuchs, B., Schiller, J., 2009. Lysophospholipids: their generation, physiological role and detection. Are they important disease markers? Mini. Rev. Med. Chem. 9, 368–378.
Glynn, P., et al., 1998. Neuropathy target esterase: immunolocalization to neuronal cell bodies and axons. Neuroscience. 83, 295–302.
Han, J., Kaufman, R.J., 2016. The role of ER stress in lipid metabolism and lipotoxicity. J. Lipid Res. 57, 1329–1338.
Herrema, H., et al., 2016. XBP1s is an anti-lipogenic protein. J. Biol. Chem. 291, 17394–17404.
Hetz, C., Mollereau, B., 2014. Disturbance of endoplasmic reticulum proteostasis in neurodegenerative diseases. Nat. Rev. Neurosci. 15, 233–249.
Hojmann Larsen, A., et al., 2001. Upregulation of the SERCA-type Ca2+ pump activity in response to endoplasmic reticulum stress in PC12 cells. BMC Biochem. 2, 4.
Jiang, H., et al., 2013a. Natalisin, a tachykinin-like signaling system, regulates sexual activity and fecundity in insects. Proc. Natl. Acad. Sci. U. S. A. 110, E3526–E3534.
Jiang, H., et al., 2013b. Natalisin, a tachykinin-like signaling system, regulates sexual activity and fecundity in insects. Proc. Natl. Acad. Sci. U. S. A. 110, E3526–E3534.
Jiang, D., et al., 2015. Targeting the IRE1α-XBP1 branch of the unfolded protein response in human diseases. Semin. Cancer Biol. 33, 48–56.
Kakisaka, K., et al., 2012. Mechanisms of lysophosphatidylcholine-induced hepatocyte lipoapoptosis. Am. J. Physiol. Gastrointest. Liver Physiol. 302, G77–G84.
Kang, S., et al., 2016. Small molecular allosteric activator of the Sarco/endoplasmic reticulum Ca(2+)-ATPase (SERCA) attenuates diabetes and metabolic disorders. J. Biol. Chem. 291, 5185–5198.
Kienesberger, P.C., et al., 2009. Mammalian patatin domain containing proteins: a family with diverse lipolytic activities involved in multiple biological functions. J. Lipid Res. 50, S63–S68 Suppl.
Kim, R., et al., 2006. Role of the unfolded protein response in cell death. Apoptosis 11, 5–13.
Kinghorn, K.J., et al., 2015. Loss of PLA2G6 leads to elevated mitochondrial lipid peroxidation and mitochondrial dysfunction. Brain. 138, 1801–1816.
Kmoch, S., et al., 2015. Mutations in PNPLA6 are linked to photoreceptor degeneration and various forms of childhood blindness. Nat. Commun. 6, 5614.
Kretzschmar, D., et al., 1997. The swiss cheese mutant causes glial hyperwrapping and brain degeneration in Drosophila. J. Neurosci. 17, 7425–7432.
Lagace, T.A., Ridgway, N.D., 2013. The role of phospholipids in the biological activity and structure of the endoplasmic reticulum. Biochim. Biophys. Acta 1833, 2499–2510.
Lauwers, E., et al., 2016. Membrane lipids in presynaptic function and disease. Neuron 90, 11–25.
Lin, P., Ye, R.D., 2003. The lysophospholipid receptor G2A activates a specific combination of G proteins and promotes apoptosis. J. Biol. Chem. 278, 14379–14386.
Lush, M.J., et al., 1998. Neuropathy target esterase and a homologous Drosophila neurodegeneration-associated mutant protein contain a novel domain conserved from bacteria to man. Biochem. J. 332 (Pt 1), 1–4.
Masuyama, K., et al., 2012. Mapping neural circuits with activity-dependent nuclear import of a transcription factor. J. Neurogenet. 26, 89–102.
McFerrin, J., et al., 2017. NTE/PNPLA6 is Expressed in Mature Schwann cells and is Required for Glial Ensheathment of Remak Fibers. vol. 65. pp. 804–816.
Mei, Y., et al., 2013. Endoplasmic reticulum stress and related pathological processes. J. Pharmacol. Biomed. Anal. 1, 1000107.
Moser, M., et al., 2000. Cloning and expression of the murine sws/NTE gene. Mech. Dev. 90, 279–282.
Moser, M., et al., 2004. Placental failure and impaired vasculogenesis result in embryonic lethality for neuropathy target esterase-deficient mice. Mol. Cell. Biol. 24, 1667–1679.
Muhlig-Versen, M., et al., 2005. Loss of Swiss cheese/neuropathy target esterase activity causes disruption of phosphatidylcholine homeostasis and neuronal and glial death in adult Drosophila. J. Neurosci. 25, 2865–2873.

Paran, C.W., et al., 2015. Lipogenesis mitigates dysregulated sarcoplasmic reticulum calcium uptake in muscular dystrophy. Biochim. Biophys. Acta 1851, 1530–1538.
Parks, J.S., Gebre, A.K., 1997. Long-chain polyunsaturated fatty acids in the sn-2 position of phosphatidylcholine decrease the stability of recombinant high density lipoprotein apolipoprotein A-I and the activation energy of the lecithin:cholesterol acyltransferase reaction. J. Lipid Res. 38, 266–275.
Paschen, W., Mengesdorf, T., 2005. Endoplasmic reticulum stress response and neurodegeneration. Cell Calcium 38, 409–415.
Pinton, P., et al., 2008. Calcium and apoptosis: ER-mitochondria Ca2+ transfer in the control of apoptosis. Oncogene. 27, 6407–6418.
Quistad, G.B., et al., 2003. Evidence that mouse brain neuropathy target esterase is a lysophospholipase. Proc. Natl. Acad. Sci. U. S. A. 100, 7983–7987.
Rainier, S., et al., 2011. Motor neuron disease due to neuropathy target esterase gene mutation: clinical features of the index families. Muscle Nerve 43, 19–25.
Ramanadham, S., et al., 2015. Calcium-independent phospholipases A2 and their roles in biological processes and diseases. J. Lipid Res. 56, 1643–1668.
Read, D.J., et al., 2009. Neuropathy target esterase is required for adult vertebrate axon maintenance. J. Neurosci. 29, 11594–11600.
Ritz, E., et al., 1980. Phosphate, calcium and lipid metabolism. Adv. Exp. Med. Biol. 128, 197–208.
Rodrigues, C.M., et al., 2003. Tauroursodeoxycholic acid prevents Bax-induced membrane perturbation and cytochrome C release in isolated mitochondria. Biochemistry 42, 3070–3080.
Roussel, B.D., et al., 2013. Endoplasmic reticulum dysfunction in neurological disease. Lancet Neurol. 12, 105–118.
Schindelin, J., et al., 2012. Fiji: an open-source platform for biological-image analysis. Nat. Methods 9, 676–682.
Schoemaker, M.H., et al., 2004. Tauroursodeoxycholic acid protects rat hepatocytes from bile acid-induced apoptosis via activation of survival pathways. Hepatology. 39, 1563–1573.
Strauss, R., Heisenberg, M., 1993. A higher control center of locomotor behavior in the Drosophila brain. J. Neurosci. 13, 1852–1861.
Sunderhaus, E.R., Kretzschmar, D., 2016. Mass histology to quantify neurodegeneration in Drosophila. J. Vis. Exp. 118, e54809.
Synofzik, M., et al., 2014. PNPLA6 mutations cause Boucher-Neuhauser and Gordon Holmes syndromes as part of a broad neurodegenerative spectrum. Brain 137, 69–77.
Topaloglu, A.K., et al., 2014. Loss-of-function mutations in PNPLA6 encoding neuropathy target esterase underlie pubertal failure and neurological deficits in Gordon Holmes syndrome. J. Clin. Endocrinol. Metab. 99, E2067–E2075.
Tsuda, L., et al., 2017. Pyroglutamate–amyloid-β peptide expression in Drosophila leads to caspase-dependent and endoplasmic reticulum stress–related progressive neurodegeneration. Hum. Mol. Genet. 26, 4642–4656.
van Tienhoven, M., et al., 2002. Human neuropathy target esterase catalyzes hydrolysis of membrane lipids. J. Biol. Chem. 277, 20942–20948.
Vang, S., et al., 2014. The unexpected uses of Urso- and Tauroursodeoxycholic acid in the treatment of non-liver diseases. Glob. Adv. Health Med. 3, 58–69.
Velasco, M., et al., 2017. Lysophosphatidic acid receptors (LPARs): potential targets for the treatment of neuropathic pain. Neuropharmacology. 113, 608–617.
Verkhratsky, A., 2005. Physiology and pathophysiology of the calcium store in the endoplasmic reticulum of neurons. Physiol. Rev. 85, 201–279.
Wang, A., Dennis, E.A., 1999. Mammalian lysophospholipases. Biochim. Biophys. Acta 1439, 1–16.
Wang, M., et al., 2009. Role of the unfolded protein response regulator GRP78/BiP in development, cancer, and neurological disorders. Antioxid. Redox Signal. 11, 2307–2316.
Wang, Y., et al., 2016. TRPC1/TRPC3 channels mediate lysophosphatidylcholine-induced apoptosis in cultured human coronary artery smooth muscles cells. Oncotarget. 7, 50937–50951.
Wu, R., et al., 2015. Involvement of the IRE1α-XBP1 pathway and XBP1s-dependent transcriptional reprogramming in metabolic diseases. DNA Cell Biol. 34, 6–18.